THE ASTROPHYSICAL JOURNAL, 285:571–579, 1984 October 15

COORDINATED MULTIFREQUENCY OBSERVATIONS OF THE BL LACERTAE OBJECTS MRK 180 AND MRK 501

S. L. MUFSON[1, 2] AND D. J. HUTTER[2]
Astronomy Department, Indiana University
K. R. HACKNEY[1] AND R. L. HACKNEY[1]
Department of Physics and Astronomy, Western Kentucky University
C. M. URRY[1] AND R. F. MUSHOTZKY[1]
Laboratory for High Energy Astrophysics, NASA/Goddard Space Flight Center
Y. KONDO[1]
Laboratory for Astronomy and Solar Physics, NASA/Goddard Space Flight Center
W. Z. WIŚNIEWSKI
Lunar and Planetary Laboratory, University of Arizona
AND
H. D. ALLER, M. F. ALLER, AND P. E. HODGE
Department of Astronomy, University of Michigan
Received 1983 May 18; accepted 1984 April 30

ABSTRACT

Coordinated observations of the nearby BL Lac objects Mrk 180 and Mrk 501 have been obtained at X-ray, ultraviolet, optical, and radio wavelengths. We present for each of these sources a set of observations which gives a time-frozen picture of its continuous spectrum from the X-ray to the radio. Our time-frozen spectra of Mrk 180 and Mrk 501 have been fitted with two different models: spherically symmetric, synchrotron self-Compton models and relativistic jet models. We find that both models can account for our spectral observations. Also, both models show that the X-ray emission from these BL Lac objects is synchrotron, rather than self-Compton emission.

Although both models provide an adequate description of the data, we find the SSC models are very dependent on uncertain observational parameters and rather unphysical assumptions. We therefore conclude that jet models lead to a better understanding of our data. We discuss the implications of our model fits.

Subject headings: BL Lacertae objects — radiation mechanisms — radio sources: general — ultraviolet: spectra — X-rays: sources

I. INTRODUCTION

Studies of active galactic nuclei (AGNs) over the past 20 years have shown them to be complex, multicomponent systems which are most likely powered by a central black hole engine (Osterbrock 1978; Rees 1977). One component of most AGNs is a core region of relativistic particles and magnetic field which emits strong nonthermal radiation. In BL Lac objects, this nonthermal radiation dominates the emission from all other nuclear components. Consequently, by carefully investigating the continuum spectra of BL Lac objects, we can learn about the processes and conditions within the nonthermal emission region of AGNs.

In this paper we present coordinated multifrequency (X-ray, UV, optical, and radio) observations of two BL Lac objects: Mrk 180 and Mrk 501. Since BL Lac objects are known to vary, it was necessary to plan coordinated observations in order to obtain single-epoch snapshots, or time-frozen spectra, of the emission at many different wavelengths. The two sources investigated in our program were chosen because they were at the time among the handful of BL Lac objects that had been detected at X-ray wavelengths (Schwartz *et al.* 1978; Forman *et al.* 1978; Mushotzky *et al.* 1978; Mufson and Hutter 1981). This meant that time-frozen spectra could be obtained over the large wavelength interval from the X-ray to the radio.

[1] Guest Observer with the *International Ultraviolet Explorer* satellite.
[2] Guest Observer with the *HEAO 2* satellite.

Both Mrk 180 and Mrk 501 are relatively nearby ($z = 0.046$ and 0.034, respectively) composite systems in which a moderately luminous ($L \approx 10^{44}$ ergs s^{-1} in the range 10^9–10^{18} Hz) BL Lac object is found at the core of an elliptical galaxy (Ulrich 1978*a*; Ulrich *et al.* 1975). The AGNs were classified as BL Lac objects because of the absence of emission lines in their spectra (Ulrich 1978*a*; Ulrich *et al.* 1975), their linearly polarized optical continuum emission (Angel and Stockman 1980; Maza, Martin, and Angel 1978), and their flat power-law radio spectra (Kojoian *et al.* 1976; Ulrich *et al.* 1975). Mrk 501 is variable in the X-ray (Mushotzky *et al.* 1978; Kondo *et ál.* 1981), but relatively steady in the optical (Barbieri and Romano 1977; McGimsey and Miller 1978) and in the radio (Kojoian *et al.* 1976). As we show below, Mrk 180 is more strongly variable than Mrk 501 at all but optical wavelengths, where it too is relatively steady.

Details of the observations and analysis are given in § II, the model fitting and interpretation are discussed in § III, and the conclusions are stated in § IV.

II. OBSERVATIONS AND ANALYSIS

a) X-Ray Regime

The X-ray data reported in this paper were obtained by the imaging proportional counter (IPC) and the monitor proportional counter (MPC) aboard the *HEAO 2* satellite

(Giacconi *et al.* 1979). The IPC, which is a soft X-ray (0.15–4.5 keV) imaging detector, and the MPC, which is a harder X-ray (1–20 keV) proportional counter, observe the image field concurrently. Since both the Mrk 180 and Mrk 501 IPC fields have strong, bright X-ray sources within 1′ of the optical position of their galactic nuclei, we are confident that the BL Lac objects are X-ray sources. The absence of other strong X-ray sources in the IPC fields argues that the MPC flux we observed also comes from the BL Lac objects.

In Table 1 we give the dates and count rates [(source − background)/effective exposure time] for all the X-ray observations. The errors in the count rates are 1 sigma photon counting errors. From this table we see that Mrk 501 is brighter than Mrk 180 in both the IPC and MPC. This difference can be attributed almost entirely to the fact that Mrk 180 is farther away than Mrk 501. We find that the X-ray luminosities of both BL Lac objects are comparable once this effect is taken into account. We also find from Table 1 that both sources show significant variability on time scales of 6 months to 1 yr, behavior which is typical of BL Lac objects. Mrk 180 varies by a factor of 2 in that time interval, while Mrk 501 varies by a more modest 20% in the IPC and 50% in the MPC. It is difficult to assess whether these variations are real, since grain variations in the IPC between two exposures can introduce significant systematic errors. However, since the intensity of the off-center weak sources in the Mrk 180 IPC field remained constant between observations, the X-ray variations in Mrk 180 (at field center) are probably real. Those in Mrk 501 are smaller, and so their reality is more suspect. There is no evidence in either source of intra-observation variability as large as 20% on time scales of approximately 1000 s.

In Table 1 we also give the results of spectral fits to the IPC and MPC data. The spectral fits are all of the form

$$S_\nu = S_0(\nu/4.84 \times 10^{17})^{-\alpha} \exp\,[-N_H \sigma(E)]\ ,$$

where S_0 is the normalization constant at 2 keV in Jy, α is the energy spectral index, N_H is the hydrogen column density in cm^{-2}, and $\sigma(E)$ is the composite photoelectric absorption coefficient of the interstellar gas as calculated by Brown and Gould (1970). In making the IPC fits, allowance was made both for variations between the calculated and true IPC calibration, and for the dead-time correction caused by discharge events. For the second Mrk 180 observation, the source was so weak and the spectrum so steep that an MPC fit was not possible. In Table 1 we list the energy range over which the fit was made, the two fit parameters α and N_H, the normalization constant S_0, and the reduced χ^2, or goodness-of-fit parameter, χ^2/d.o.f. For the IPC the errors given are 90% confidence intervals calculated using the χ^2 limits found in Avni (1976). A zero in the N_H error limit means that the 90% confidence limit is consistent with no hydrogen in the line of sight. As can be seen from the goodness-of-fit parameter in the last column, all the fits have χ^2/d.o.f. $\lesssim 1.5$ and so are acceptable (Bevington 1969).

Heiles (1975) has measured N_H in the direction of Mrk 180 ($\log N_H = 20.34$) and Mrk 501 ($\log N_H = 20.52$). From Table 1 we find that these observed values are in general agreement with the column densities we calculate from our fits to the X-ray data. Only our 1979 November MPC column density for Mrk 180 is substantially different. But Mrk 180 is weak and soft, so that this determination is very uncertain.

For Mrk 180, the 2–6 keV flux derived from the MPC observation of 1979 November is 1.1×10^{-11} ergs cm^{-2} s^{-1}. For Mrk 501, the 2–6 keV fluxes are 2.4×10^{-11} ergs cm^{-2} s^{-1} for 1980 January and 3.5×10^{-11} ergs cm^{-2} s^{-1} for 1980 August. We estimate that errors in all these quoted fluxes are of the order of 25%. The 2–6 keV luminosity of both nuclei then is of the order of $L(2\text{–}6\ \text{keV}) \approx 10^{44}$ ergs s^{-1} ($H_0 = 50$ km s^{-1} Mpc^{-1}). Archival measurements of the 2–6 keV flux from Mrk 501 show that the variability we observed is rather typical behavior for this source. The *HEAO 1 A-2* values for 1978 August–September of $2.9(+1.0, -0.5) \times 10^{-11}$ ergs cm^{-2} s^{-1} (Kondo *et al.* 1981) and for 1977 August of 3.1×10^{-11} ergs cm^{-2} s^{-1} (Mushotzky *et al.* 1978); the *HEAO 1 A-3* value from 1977 August of $(3.6 \pm 1.2) \times 10^{-11}$ ergs cm^{-2} s^{-1} (Schwartz *et al.* 1978); the revised *Uhuru* value of $(2.75 \pm 0.52) \times 10^{-11}$ ergs cm^{-2} s^{-1} (Forman *et al.* 1978); and the *Ariel 5* results from 1975 March of $(3.6 \pm 1.8) \times 10^{-11}$ ergs cm^{-2} s^{-1} (Snijders *et al.* 1979) are all consistent with the fluxes we measured.

It has been suggested (Mushotzky *et al.* 1978; Worrall *et al.* 1981) that BL Lac objects like Mrk 180 and Mrk 501 have two-component X-ray spectra, and that variations in the X-ray intensity seen in some of these sources can be attributed to a fluctuating hard component superposed on a relatively constant low-energy component which extends from about 2 keV to lower energies. The X-ray spectra of both Mrk 180 and Mrk 501 show no evidence for this fluctuating hard component. In fact, the 1980 August X-ray spectrum of Mrk 501 (see Fig. 2*b*) seems to be steepening at higher energies, a result also found by

TABLE 1

X-RAY OBSERVATIONS

UT Date	Detector	Count Rate[a] (counts s^{-1})	Spectral Fit Range (keV)	Spectral Index α	log N_H (cm^{-2})	log S_0 (Jy)	χ^2/d.o.f.
			Markarian 180				
1979 Nov 13	IPC	2.68 ± 0.03	0.5–2.8	$1.3^{+0.3}_{-0.2}$	20.4 ± 0.1	-5.43 ± 0.03	1.1/4
	MPC	1.21 ± 0.05	1.1–6.6	2.9 ± 0.8	$22.2^{+0.3}_{-0.6}$	-5.18 ± 0.06	2.0/3
1980 Dec 28	IPC	1.16 ± 0.02	0.5–4.6	$0.7^{+1.0}_{-0.2}$	$19.6^{+1.0}_{-0.0}$	-5.55 ± 0.05	1.7/7
	MPC	0.45 ± 0.03	...	...	...	...	...
			Markarian 501				
1980 Jan 19/20	IPC	3.59 ± 0.03	0.3–3.4	1.4 ± 0.2	20.5 ± 0.2	-5.28 ± 0.03	10.4/8
	MPC	2.20 ± 0.04	1.1–9.7	1.5 ± 0.2	21.0 ± 0.6	-5.23 ± 0.01	2.3/4
1980 Aug 15	IPC	4.26 ± 0.05	0.3–5.3	$0.8^{+0.5}_{-0.2}$	$20.3^{+0.3}_{-0.2}$	-5.02 ± 0.03	10.4/8
	MPC	3.28 ± 0.07	1.1–9.7	1.7 ± 0.3	$21.3^{+0.2}_{-0.8}$	-4.96 ± 0.07	3.4/4

[a] For IPC, count rate is over entire bandpass, nominally 0.15–4.5 keV; for MPC, count rate is for 1.1–6.6 keV bandpass.

Kondo *et al.* (1981). Since this high-energy component appears only 20% of the time, however, it is possible that our observations were made during times when the hard spectral component was absent.

b) Ultraviolet Regime

The ultraviolet observations were obtained between 1978 and 1981 using the *IUE* satellite (instrumentation described by Boggess *et al.* 1978*a*, *b*). Spectral observations were made in the low-dispersion mode (effective resolution approximately 10 Å) with both the SWP (1150–1950 Å bandpass) and LWR (1900–3200 Å bandpass) cameras. Spectral images were assembled from geometrically and photometrically rectified data samples in the line-by-line files of the *IUE* Guest Observer tapes. For tapes written with the erroneous SWP intensity function in use early in the *IUE* project, corrections were applied using the algorithm of Cassatella *et al.* (1980) (3 Agency 4th file method) with quadratic interpolation of the samples to recover data at pixel resolution (Holm and Schiffer 1980).

During exposures of several hours on faint objects, like our images of Mrk 501 and Mrk 180, significant backgrounds amounting to one-sixth to one-half the gross exposure level can build up. In such high-background *IUE* images of faint targets, several factors in addition to photon statistics contribute noise to the extracted spectra (Hackney, Hackney, and Kondo 1982, 1984). In particular, radiation events of random intensity and location may affect pixels or groups of pixels; fixed-pattern noise structures may be present in the spectra (these are apparently due to factors inherent in the pixel sampling and the pixel-by-pixel application of the intensity transfer function); adjacent data elements in extracted spectra may appear correlated over several samples, resulting in apparent low-contrast spectral features that persist even in blank field exposures; and finally, there may be systematic effects, such as nonlinearity of the photometrically corrected responses of both cameras (Holm 1982), which can be seen upon comparing calibration spectra exposed to various gross signal levels. These nonlinear effects are exacerbated by the varying levels of background over the image field generated during long-duration exposures of faint objects. In addition, there are residual artifacts in the shape of the SWP spectra that are not simple calibration errors and which cannot be satisfactorily corrected at this time (Hackney, Hackney, and Kondo 1982). All these shape and nonlinearity errors affect spectral shapes, slopes, and flux levels, causing discrepancies between SWP and LWR images, even when taken in quick succession. In the *IUE* spectral images of Mrk 180 and Mrk 501, the amplitude of the residual instrumental profile is approximately 10% of the indicated mean flux level.

An effort was made to reduce nonsystematic noise effects in the spectral images taken from the Guest Observer tapes. For the present study, the spectra were extracted from the line-by-line files by fitting a Gaussian point-spread function to cross-cuts perpendicular to the direction of spectral dispersion (after Koorneef and de Boer 1979; Panek 1983). Nonlinear least squares fits were then performed (Bevington 1969), with the background base level, the integrated signal in the profile, the location of the center of light, and the dispersion of the Gaussian function as free parameters. Filtering for radiation events was accomplished by first rejecting points which deviated more than two standard deviations from the profile, and then iterating the fit. The final extraction was made during a second pass in which the dispersion of the Gaussian was forced to the value given by a linear regression of the sample dispersion estimates obtained in the initial pass.

The resulting spectra were calibrated to absolute fluxes using the 1980 May project calibration (Bohlin and Holm 1980). Errors in the calibration are estimated to be no greater than 10% when applied to low-background images of bright stars. We applied no correction for interstellar reddening because of the high galactic latitudes of the sources (Mrk 180: 45°6; Mrk 501: 38°8) and the predictions for the individual lines of sight (Burstein and Heiles 1978). Prior to the least squares fitting of a power-law function to the continuum, the data were binned by averaging consecutive points (100 Å bins in LWR, 50 Å bins in SWP). In performing the least squares fit, the bin means were weighted individually according to the inverse square of their standard deviation. With these Gaussian fitting and filtering procedures, there resulted a notable reduction in the scatter of the power-law spectral indices estimated for repeated exposures of Mrk 501, compared with the results of initially extracting the images using the recommended summation procedure (Turnrose and Harvel 1980).

The improved continuum definition revealed significant image-to-image variations in the extracted LWR fluxes in the low-sensitivity region $\lambda < 2300$ Å. Apparently the nonlinearity of the camera response severely affects data in this region, since the gross exposure is only slightly above the background and large calibration corrections must be made. This behavior seems to preclude reliable independent determinations of the reddening from *IUE* images of faint targets with significant background levels, since the 2200 Å dust feature in the interstellar extinction curve is poorly defined in the LWR images. The erratic behavior of extracted LWR points with $\lambda < 2300$ Å led us to omit them from the reduced data and power-law fits. The net effect of the Gaussian fitting–filtering procedure and omission of LWR points with $\lambda < 2300$ Å was a marked reduction in the scatter of spectral indices for the Mrk 501 images. Whereas the spectral indices for fits to data extracted using the standard procedure ranged to ± 10 times the 1 σ errors indicated from the internal statistics of the fits, we now find the range reduced to about $\pm 4\,\sigma$.

There remain in the data visible effects of the SWP instrumental profile and possible nonlinearity effects that vary from exposure to exposure in both cameras (Hackney, Hackney, and Kondo 1984). These factors affect the goodness-of-fit measures for fits to each camera alone and for fits to combined LWR-SWR image pairs taken quasi-simultaneously. With the omission of LWR points with $\lambda < 2300$ Å, the systematic errors affecting the spectral indices can be partially removed.

In Table 2 we give the details of the observations. We list the date, the camera used, the *IUE* image number, the exposure time, and in the last three columns, the parameters of the spectral fits to the data. Our observations were fitted to power-law functions of the form $\log S(\mathrm{Jy}) = \log S_0 - \alpha(\log \nu - 15.2)$ using a weighted least squares technique (Bevington 1969). One sigma errors are quoted in the table. As can be seen from the column giving the goodness-of-fit parameter, there are several Mrk 501 images that are not well represented by a power law because they are apparently impressed with the systematic errors discussed above. For the single Mrk 180 SWP image, the fit is poor because of the unusually high background rate during this observation. For both sources, the spectra in Table 2 show no statistically significant variations in either the spectral index or the intensity.

In Figure 1 we show the ultraviolet spectral index of Mrk

TABLE 2

ULTRAVIOLET OBSERVATIONS

UT Date	Camera	*IUE* Image Number	Exposure Time (s)	Spectral Index α	log S_0 (Jy)	χ^2/d.o.f.
			Markarian 180			
1980 May 21	LWR	7814	10680	0.67 ± 0.37	-3.15 ± 0.06	0.66/9
1980 Nov 8	SWP	10563	25200	0.67 ± 0.07	-3.11 ± 0.01	24.0/12
1980 Nov 10	LWR	9277	15600	0.73 ± 0.28	-3.15 ± 0.05	8.2/10
			Markarian 501			
1978 Aug 25	SWP	2394	22800	0.83 ± 0.04	-2.80 ± 0.01	67.7/10
1978 Aug 26	LWR	2177	18000	1.03 ± 0.12	-2.82 ± 0.02	14.8/9
1978 Oct 24	SWP	3133	21600	0.72 ± 0.05	-2.78 ± 0.01	46.2/10
1978 Oct 27	LWR	2729	19200	1.14 ± 0.15	-2.81 ± 0.02	38.7/9
1979 Mar 2	SWP	4454	28800	0.80 ± 0.05	-2.73 ± 0.01	42.3/10
1979 Mar 26	SWP	4757	18000	0.87 ± 0.05	-2.80 ± 0.01	54.9/10
1979 Nov 14	SWP	7147	24300	0.65 ± 0.05	-2.81 ± 0.01	33.5/10
1980 Aug 30	SWP	9954	25200	0.70 ± 0.05	-2.89 ± 0.01	37.4/10
1981 Mar 7	SWP	13427	18000	0.80 ± 0.05	-2.80 ± 0.01	29.4/12

501 plotted against its flux density at 2550 Å. As is readily apparent, there is no correlation between these two quantities. Mrk 421, a BL Lac object similar in excitation to Mrk 501, also shows no correlation between these quantities (Ulrich *et al.* 1984). Such behavior is typical of BL Lac objects, but different from what is observed in Seyfert I galaxies. In Seyfert I galaxies, the ultraviolet spectrum gets harder as the source gets fainter (Ulrich *et al.* 1984). Ulrich *et al.* (1984) speculate that thermal sources present in Seyfert galaxies, but absent or weak in BL Lac objects, are responsible for this difference in behavior.

c) *Optical Regime*

The ground-based optical photometry reported here consists of broad-band *BVRI* measurements made between 1980 and 1982 using the 1 m and 1.5 m telescopes of the University of Arizona Mount Lemmon Observatory. Extinction and transformation coefficients were determined from observations of the primary *UBVRI* standards (Johnson *et al.* 1966).

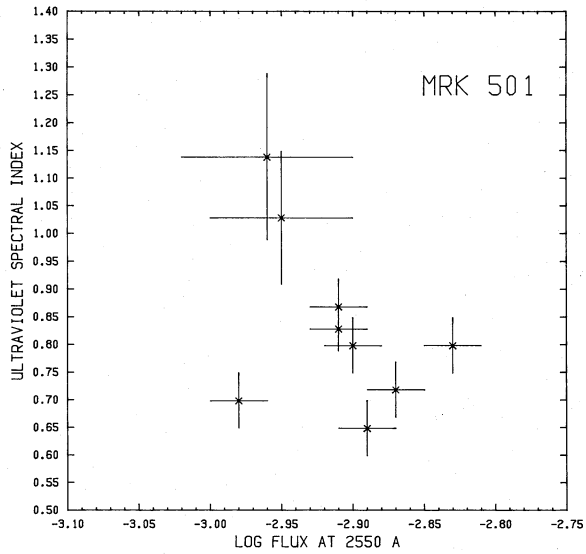

FIG. 1.—The ultraviolet spectral index for Mrk 501 plotted against the ultraviolet flux density at 2550 Å. No correlation is observed in these two quantities. This behavior is similar to what is observed in other BL Lac objects.

The results of the photometry are summarized in Table 3. Here we list the date of the observations, the telescope used, the diameter of the measuring aperture in arc seconds, and the *BVRI* magnitudes. The errors in the magnitudes are all photometric errors; the true errors are likely to be at least 50% larger (see Hutter and Mufson 1981). The magnitudes given for Mrk 180 have been corrected for the presence of a star 7″.2 from the nucleus by the method described in Mufson and Hutter (1981).

Previous observations (Barbieri and Romano 1977; McGimsey and Miller 1978) have shown that Mrk 501 does not vary strongly at optical wavelengths. The data in Table 3 are consistent with this result. The comparison of the photometric data presented here with those in Mufson and Hutter (1981) shows that Mrk 180 was also approximately constant in brightness and color over more than 7 months. Since the unvarying elliptical galaxy contributes a substantial fraction of the optical output from Mrk 180 and Mrk 501, it is not surprising that these objects remain relatively constant in the optical.

d) *Radio Regime*

In Table 4 we summarize the radio observations. The data were obtained with the University of Michigan computer-controlled 26 m radio dish. The flux densities given are means of the observations made that month weighted by their photometric errors. The number of observations used to compute the mean is given in parentheses. One sigma errors are quoted in the table.

There is little suggestion of strong variability in either Mrk 180 or Mrk 501. Archival measurements show that Mrk 501 has remained relatively constant in the centimeter region from 1980 to 1982 (Aller, Aller, and Hodge 1984).

e) *Coordinated Observations*

Since both Mrk 180 and Mrk 501 are BL Lac objects, most of which are known to vary significantly at all wavelengths, coordinated observations were necessary in order to be sure that we would get time-frozen spectra from the X-ray to the radio. For Mrk 180, the coordinated observations are those of

TABLE 3

OPTICAL OBSERVATIONS

UT Date	Telescope	Aperture Diameter	B (mag)	V (mag)	R (mag)	I (mag)
			Markarian 180[a]			
1980 Dec 30	1 m	46″	15.78 ± 0.05	14.95 ± 0.06	14.20 ± 0.06	...
			Markarian 501[b]			
1980 Aug 31	1.5 m	12″.3	14.70 ± 0.02	13.95 ± 0.02	13.17 ± 0.02	12.51 ± 0.02
		16″.8	14.61 ± 0.02	13.83 ± 0.02	13.03 ± 0.02	12.34 ± 0.02
		26″.8	14.48 ± 0.02	13.60 ± 0.02	12.79 ± 0.02	12.05 ± 0.02
1981 Aug 14	1.5 m	16″.8	14.59 ± 0.02	13.72 ± 0.02	12.92 ± 0.02	12.21 ± 0.02
1982 Jun 1	1.5 m	16″.8	14.50 ± 0.02	13.68 ± 0.02	12.91 ± 0.02	12.24 ± 0.02

[a] Magnitudes corrected for star 7″.2 south of nucelus as discussed in Mufson and Hutter 1981.
[b] All photometric errors approximately 2%.

1980 November–December. Although observations spaced only a few days apart were planned, difficulties with the *HEAO 2* satellite caused postponement of the X-ray observations for a month. The data for this period, with the X-ray data corrected for the turnover due to interstellar absorption along the line of sight, are plotted in Figure 2*a*.

At low frequencies, the radio spectrum can be fitted to the flat power law $\log S(\mathrm{Jy}) = -0.32 - 0.08(\log \nu - 10)$. Although this radio spectrum is uncertain because of the small number of data points used in the fit, we note that historically the radio spectrum of Mrk 180 has been as flat as this (Mufson and Hutter 1981). From the archival data shown on Figure 2*a* (Sramek and Tovmassian 1975; Sulentic 1976; Kojoian *et al.* 1976; Biermann *et al.* 1980), it appears that Mrk 180 was relatively bright in the radio at the time of these coordinated observations.

The coordinated observations of Mrk 501 were made during 1980 August, except in the radio, where the data are from 1981 March. Since Mrk 501 has not been strongly variable in the radio (Aller, Aller, and Hodge 1984), these later data should be reasonably accurate. The data for this period, with the X-ray data again corrected for the turnover due to absorption along the line of sight, are plotted in Figure 2*b*. The archival radio data shown on Figure 2*b* (Colla *et al.* 1975; Ghigo and Owen 1973; Owen *et al.* 1978; Owen, Spangler, and Cotten 1980; Sulentic 1976; Ulrich *et al.* 1975), when combined with our radio data, can be fitted by a simple power law of the form $\log S(\mathrm{Jy}) = 0.04 - 0.18(\log \nu - 10)$. This flat radio spectrum is typical of BL Lac objects. Also plotted in Figure 2*b* are the archival infrared data of Allen (1976) and Joyce and Simon (1976).

TABLE 4

RADIO OBSERVATIONS

Date	$S_{14.5}$ (Jy)	$S_{8.0}$ (Jy)	$S_{4.8}$ (Jy)
	Markarian 180		
1980 May	...	0.31 ± 0.02 (4)	...
1980 Nov	0.39 ± 0.08 (1)	0.54 ± 0.05 (3)	...
1981 Mar	0.43 ± 0.03 (2)[a]	0.37 ± 0.04 (2)	...
1981 Apr	0.49 ± 0.04 (1)	0.40 ± 0.03 (3)	...
	Markarian 501		
1981 Mar	1.10 ± 0.02 (6)	1.24 ± 0.03 (3)	...
1981 Apr	1.13 ± 0.03 (4)	1.31 ± 0.03 (3)	...
1982 Mar	1.08 ± 0.02 (2)	1.23 ± 0.03 (2)	1.25 ± 0.03 (3)

[a] Average of two measurements: 0.50 + 0.04 Jy and 0.31 ± 0.05 Jy, separated by 2 weeks.

III. INTERPRETATION OF THE COORDINATED OBSERVATIONS

a) The Synchrotron Self-Compton (SSC) Model

A likely explanation for the separate power laws seen in the optical-UV and radio regions of Figures 2*a* and 2*b* is provided by the synchrotron process. One simple source model which gives spectra of this type is the homogeneous synchrotron self-Compton (SSC) model (Jones, O'Dell, and Stein 1974*a*, *b*; Burbidge, Jones, and O'Dell 1974; Marscher *et al.* 1979). In this model a spherically symmetric, homogeneous volume of tangled magnetic field and relativistic electrons emits incoherent synchrotron radiation and, when the radiation density is high enough, self-Compton emission. This model can be simply modified to also include the effects of relativistic expansion (Marscher 1983).

SSC spectra can be characterized by a relatively small number of parameters. For Mrk 180 and Mrk 501 these parameters are listed in Table 5. In this table we first give the optically thin spectral index, α_r, which we have taken from the radio region of the spectrum. Since the spectra of Mrk 180 and Mrk 501 show no evidence for a low-frequency turnover, we are constrained in this homogeneous, single-component model to identify the optically thin emission with the low-frequency radio emission. We next give the turnover frequency, ν_m, and the flux density at the turnover, S_m. Because no low-frequency turnover is seen, the values of ν_m and S_m we quote are taken from the lowest frequency at which the spectrum has been

TABLE 5

SYNCHROTRON SELF-COMPTON MODELS FOR MRK 180 AND MRK 501

Parameter	Mrk 180	Mrk 501
α_r	0.08	0.18
ν_m[a] (GHz)	$\lesssim 2.8$	$\lesssim 0.708$
S_m (Jy)	$\gtrsim 0.5$	$\gtrsim 1.8$
ν_b (GHz)	150	190
α_{UV}	0.67	0.69
θ (mas)	0.5	2
B (G)	$\lesssim 4.3 \times 10^{-4}$	$\lesssim 8.8 \times 10^{-6}$
$[S^C(2\ \mathrm{keV})]_{\mathrm{pred}}$ (Jy)	$\gtrsim 2.3 \times 10^{-5}$	$\gtrsim 1.2 \times 10^{-3}$
$[S(2\ \mathrm{keV})]_{\mathrm{obs}}$ (Jy)	3.2×10^{-6}	2.5×10^{-6}

[a] Lowest frequency at which flat radio spectrum is observed.

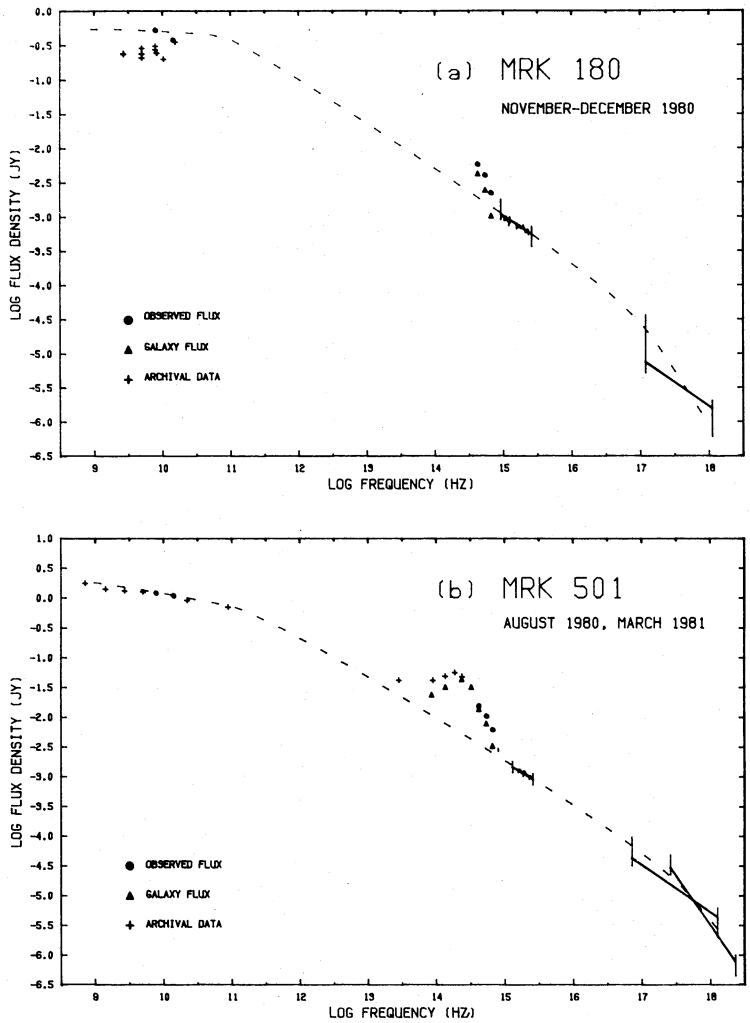

FIG. 2.—(*a*) The multifrequency spectrum of Mrk 180 from the observations of 1980 November–December. The observed ultraviolet and X-ray (IPC) data are shown as solid lines flanked by error bars. The optical fluxes, which are shown as solid circles, have been decomposed into galactic and nonthermal components by the methods described in the text. The dashed curves give the best fitting relativistic jet model. (*b*) The multifrequency spectrum of Mrk 501 from the observations of 1980 August. The radio data come from 1981 March. As above, the ultraviolet and X-ray (IPC and MPC) data are shown as solid lines. The decomposition of the optical fluxes is also shown. The best fitting relativistic jet model is displayed as a dashed line. In this figure the galaxy model has been projected into the infrared using the colors of Whitford (1975).

measured. This makes ν_m an upper limit and S_m a lower limit. The next two parameters we give in Table 5 are ν_b, the break frequency above which the effects of synchrotron losses become important, and α_{UV}, the spectral index of the emission above ν_b. The value of α_{UV} is taken from the ultraviolet data, where we are unquestionably seeing optically thin synchrotron emission uncontaminated by galaxy emission. The value of ν_b is derived from the intersection of the UV and radio power laws. In the simple SSC model we are describing here, the difference between the spectral index above and below should be 0.5. Both Mrk 180 and Mrk 501 are consistent with this result.

Another parameter which is needed in the description of an SSC model is the angular size of the source, θ. For Mrk 180, which has not been measured by *VLBI* techniques, we have taken θ to be the metric diameter of the source as determined from the variability time scale. In the limit $z \ll 1$,

$$\theta = \frac{2tH_0\,\delta}{z} = 0.021\,\frac{t_v(\mathrm{yr})\delta}{z}\left(\frac{H_0}{50}\right)\text{milli-arcsec}\,, \qquad (1)$$

where $t_v = |d \ln S_v/dt|^{-1}$ is the variability time scale, $H_0 = 50$ km s^{-1} Mpc^{-1}, δ = Doppler enhancement factor due to bulk relativistic motion (see eq. [2]), and the expression is valid for all q_0 (Sandage 1975; Burbidge, Jones, and O'Dell 1973). The value of θ is listed in Table 5. For Mrk 180, the radio and X-ray variability time scales are consistent with one another and approximately equal to 1 yr. This gives a source size of 0.5 mas at both X-ray and radio wavelengths. For Mrk 501, we have taken $\theta = 2$ mas, which is a factor of 1.8 times the *VLBI* half-width given by Weiler and Johnston (1980). The additional factor of 1.8 corrects the observed Gaussian full width half-maximum angular size to the true source diameter (Marscher 1983). We have also computed for this source variability time scales using the X-ray data in Table 1 and the ultraviolet data in Table 2. We found that both variability time scales correspond to approximately 2.2 mas, a value quite close to the *VLBI* size. The similarity of all these sizes shows that Mrk 501 has emitting volumes which are roughly coextensive at all wavelengths, as required by the SSC model.

We can use standard formulae (Marscher 1983) with the parameters in Table 5 to estimate the magnetic field strength, B, and the self-Compton flux at 2 keV, $S^C(2\text{ keV})$, for our sources. The results of these calculations, assuming that the source is not expanding relativistically ($\delta = 1$), are given in Table 5. In this table we also give the observed 2 keV flux density. It is apparent that the SSC model predicts self-Compton emission far in excess of what is observed at 2 keV. However, the calculations depend critically on the uncertain source size raised to a high power. Consequently, a small change in θ can lead to a large change in the calculated self-Compton flux, thus providing an explanation for the difference in the observed and predicted 2 keV flux. In addition, we could reduce the predicted self-Compton emission sufficiently by allowing the sources to expand relativistically (with Doppler factors of $\delta = 1.6$ for Mrk 180 and $\delta = 4.1$ for Mrk 501). We conclude, then, that the SSC model can be made to work for our observations of Mrk 180 and Mrk 501.

However, even though we can build SSC models that describe our observations, there are still problems. For instance, some of the parameters on which the model depends strongly, like the source size and the synchrotron self-absorption turnover frequency, are not well determined at all. This leads to an uncomfortably large range of possible model solutions and derived physical parameters. In addition, "normal" synchrotron sources have optically thin radio spectra which are considerably steeper than we found here. The flat radio spectra observed in compact radio sources like Mrk 180 and Mrk 501 are ordinarily ascribed to inhomogeneities in the source (Condon and Dressel 1973; de Bruyn 1976), rather than to the optically thin region of a homogeneous synchrotron spectrum. With these problems in mind we describe in the following section a model in which the source size does not enter explicitly, the turnover frequency is determined as a result of the fitting procedure, and the flat radio spectrum naturally arises from inhomogeneities in the source.

b) *Inhomogeneous Jet Models for Mrk 180 and Mrk 501*

In this section we use a jet model to describe our source spectra. We have chosen the jet model because it relaxes the assumptions that the source be spherical and homogeneous, it does not use the source size explicitly, and it allows for relativistic expansion. One reason for selecting this particular source geometry is the growing body of evidence suggesting that jetlike features are common in AGNs (Kellermann and Pauliny-Toth 1981).

The relativistic jet model we have used is a modified version of the one found in Blandford and Königl (1979) and Königl (1981). The model has been modified by including a more precise calculation of the self-Compton emission (Baylis, Schmid, and Lüscher 1967). A fuller description of our model can be found in Hutter (1982). The jet itself is a cone of half-angle ϕ, the axis of which is inclined at an angle ψ to the line of sight. Relativistic particles and field move outward through this jet in simple ballistic motion with relativistic velocity $\beta_j = v_j/c$ at all radial distances r from the jet apex (a free jet). It is further assumed that there is no pressure confining the jet so that it expands at the speed of sound in the direction perpendicular to the jet axis. In the rest frame of the material moving in the jet, each emitting volume consists of an isotropic population of relativistic electrons (and protons) embedded in a well-tangled magnetic field. The distribution of electrons as a function of distance r along the jet axis and energy E has the form $N_e(E, r) = N_0 E^{-2(\alpha+1)} r^{-n}$ cm^{-3}, where α is the spectral index of the optically thin incoherent synchrotron radiation. To prevent a divergence in the particle number, the electron distribution is nonzero only in the range $E_l \leq E \leq E_u$. The magnetic field strength along the jet axis is $B(r) = B_0 r^{-m}$ G. In the fluid frame we assume that the electrons emit isotropic incoherent synchrotron radiation (Ginzburg and Syrovatskii 1965; Moffet 1975). We calculated the self-Compton emission by assuming that only one local scattering occurs before a synchrotron photon escapes. The frequency spectrum of the Compton-scattered radiation is computed from Baylis, Schmid, and Lüscher (1967). The total flux density of radiation observed at frequency ν is

$$S_{\rm obs}(\nu) \approx 3 \times 10^{41} \left[\frac{(1+z)\delta^2}{D^2}\right] \int_{r_{\rm min}}^{r_{\rm max}} \epsilon'(\nu')\pi(r\phi)^2 dr \text{ Jy}, \quad (2)$$

where $\delta = (1-\beta_j^2)^{-1/2}(1-\beta_j \cos\psi)^{-1}$ is the Doppler enhancement factor, $D = cz/H_0$ is the distance to the source, $\epsilon' = \epsilon_s' + \epsilon_C'$ is the synchrotron plus self-Compton emission in the fluid frame at the frequency $\nu' = \nu(1+z)/\delta$. The factor $\pi(r\phi)^2$ is a geometric factor derived from the jet geometry, and $r_{\rm min}$ and $r_{\rm max}$ are the inner and outer radii, respectively, of the portion of the jet that emits optically thin synchrotron emission. The procedure for evaluating this complicated integral is described in Hutter (1982).

A best fitting model was determined by fixing four parameters, and then minimizing χ^2 with respect to the remaining free parameters. The optical-UV and radio power-law spectra were fixed according to the results of § II*d*. In addition, the local optically thin spectral index in the fluid frame for both Mrk 180 and Mrk 501 was set to 0.5, a value which both prevents the integral in equation (2) from diverging and ensures that N_e and B do not increase with increasing distance along the jet axis, an unphysical result. Also, values of ϕ and ψ were chosen so that the model self-Compton flux was less than 1% of the model synchrotron flux at $\log \nu = 17.684$. Once the values of these four quantities were specified, initial guesses were made at the four fit parameters ν_M, $S(\nu_M)$, R_V, and $\nu_{\rm min}$, where ν_M is the highest frequency at which an element of the jet becomes optically thick to synchrotron radiation, $S(\nu_M)$ is the flux density at ν_M, $R_V = S_{\rm nt}/S_{\rm gal}$ is the ratio of nonthermal flux to galactic flux (or the contamination factor) in the V bandpass, and $\nu_{\rm min}$ is the lowest frequency of synchrotron emission. In Figures 2*a* and 2*b*, ν_M is the frequency at which the radio spectra become flat. The minimization program then found the set of parameters which could best describe the Mrk 180 and Mrk 501 spectra. The parameters of this fit are given in Table 6.

As can be seen in Figures 2*a* and 2*b*, the calculated model spectra reproduce most features of the observed Mrk 180 and Mrk 501 spectra. Several aspects of these models should be noted. First, the superposition of the many different synchrotron spectra from different regions along the jet produces a composite spectrum with a flat radio spectral index, nearly independent of the optical-UV spectral index. This is the typical behavior of an inhomogeneous synchrotron source (Condon and Dressel 1973; de Bruyn 1976). Second, the optical-UV spectrum has a continuously varying spectral index without a break frequency because each emitting volume making a contribution to the observed flux has a different break frequency, depending upon its location in the jet. We can characterize the nonthermal spectra of both Mrk 180 and Mrk 501 in the optical by an approximate spectral index of $\alpha = 0.70$.

TABLE 6

INHOMOGENEOUS JET MODELS FOR MRK 180 AND MRK 501

Parameter	Mrk 180	Mrk 501
$\phi = (1-\beta_j^2)^{-1/2}$ (rad)	0.1	0.1
ψ (rad)	0.3	0.4
ν_M (Hz)	7.5×10^{10}	1.3×10^{11}
$S(\nu_M)$ (Jy)	0.5	0.8
$R_V = (S_{nt}/S_{gal})_V$	0.67[a]	0.33[b]
δ	2.0	1.1
n	1.1	1.6
K_e(1 pc)[c]	55	140
m	1.6	1.1
B(1 pc)	6.4×10^{-2}	9×10^{-2}
r_{min} (pc)	0.09	0.03
r_{max} (pc)	345	3240

[a] Through a 46″ aperture.
[b] Through a 16″.8 aperture.
[c] $K_e(r) = \int_{E_l}^{E_u} N_e\, dE$.

The value of the spectral index we find for Mrk 501 is the same as that found by Hickson *et al.* (1982) from their CCD observations, and similar to the value of 0.8 found by Maza, Martin, and Angel (1978) from polarization studies. The value of 0.0 found by Kondo *et al.* (1981) for the spectral index of Mrk 501 is significantly different from what has been obtained here. We believe the value obtained here is more reliable because it is consistent with previous results. (As an additional check on our spectral index, we have decomposed the optical magnitudes into nonthermal and galactic components using the aperture photometry in Table 3 and the method of Sandage 1973. We again find a value of 0.7.) Third, since relativistic jet motion focuses radiation emitted in a narrow beam and thereby lowers the rest frame radiation density, there is a lower self-Compton flux in these models when compared with the isotropic SSC models.

From Table 6 we find that $R_V = 0.67$ for Mrk 180 and $R_V = 0.33$ for Mrk 501. In these sources, then, the galaxy outshines the BL Lac object. For $H_0 = 50$, the absolute magnitudes of the host galaxies can be calculated to be $M_V = -21.9$ for Mrk 180 and $M_V = -22.2$ for Mrk 501. The host galaxies of these BL Lac objects are thus comparable in brightness to the giant elliptical galaxy NGC 4489 (Mihalas and Binney 1981), a first-ranked cluster elliptical. Our galaxy magnitude for Mrk 501 agrees well with that found in Kondo *et al.* (1981). The Mrk 501 galaxy magnitude found by Hickson *et al.* (1982) is approximately 1 mag brighter than our result (assuming normal elliptical galaxy colors). However, considering that Hickson *et al.* (1982) give a magnitude for the entire galaxy, and our result is only for the inner 16″.8, the two results are in reasonable agreement.

In Figure 2*b*, we have extended our Mrk 501 galaxy model into the infrared using the elliptical galaxy colors of Whitford (1975). At long infrared wavelengths, the fluxes observed are larger than predicted by the galaxy model. Although these infrared data are from different epochs, there is a suggestion that a component of infrared flux is present in addition to the flux contributed by the elliptical galaxy and the nonthermal source.

A careful examination of the model parameters in Table 6 leads to some interesting conclusions about the model jets in Mrk 180 and Mrk 501. For a jet which is free to expand adiabatically, conservation of magnetic flux and particle number predicts that N and B scale as $r^{-(2\alpha+3)}$ and r^{-2}, respectively (Moffet 1975). But as seen in Table 6, the best fit models have N falling much more slowly than this, implying that particle injection must be occurring along the jet. The necessity for distributed particle sources in jets has been pointed out by Blandford and Königl (1979) and Rees, Begelman, and Blandford (1981). In this model, the magnetic field dominates the flow at small jet radii, and the particle energy density dominates the flow at large radii. Thus the characteristics of the fluid flow changes as the fluid moves outward along the jet.

IV. CONCLUSION

We have investigated the continuous spectra of the two nearby BL Lac objects Mrk 180 and Mrk 501 by making coordinated observations at X-ray, ultraviolet, optical, and radio wavelengths. We have found that Mrk 180 and Mrk 501 can be described by a spherically symmetric, homogeneous SSC model. However, these models depend heavily on uncertain observational parameters and rather unphysical assumptions. We have therefore relaxed the assumptions of spherical geometry and homogeneity, and allowed for relativistic motion by building jet models for these sources. We find that these models provide accurate fits to the observed spectra and tighter constraints on the physical parameters. These models are also not dependent on the uncertain source size or synchrotron break frequency.

As pointed out by Urry *et al.* (1982), the relativistic jet picture predicts that $\delta \gtrsim 3$ for BL Lac objects and rapidly varying quasars, while quiescent quasars have $\delta \approx 1$. For many BL Lac objects and active quasars, such as PKS 0548−322 (Urry *et al.* 1982), 0735+178 (Bregman *et al.* 1984), 1156+295 (Glassgold *et al.* 1983), and PKS 2155−304 (Urry and Mushotzky 1982), the relativistic beaming factor is this large. But here we have two examples of BL Lac objects which do not fit into this picture. Bregman *et al.* (1982) came to a similar conclusion for the BL Lac object I Zw 187. In addition, the presence of an unresolved relativistic jet aligned nearly to the line of sight cannot be responsible for the absence of line emission in either Mrk 180 or Mrk 501. At least in these cases, an alternative explanation must be found for the BL Lac phenomenon. One possibility is that the intense nonthermal continuum radiation in these sources evaporates the line-emitting regions.

We gratefully acknowledge the assistance of the US *IUE* project team in the acquisition and reduction of the observations. We acknowledge discussions with W. Kinzel, A. Marscher, and T. Kallman. We also thank J. Blegman for helpful comments on an earlier draft of this paper. This research was supported in part by NASA grants NAG-5-198 (S. L. M.) and NSG 5238 (K. R. H., R. L. H.).

REFERENCES

Allen, D. A. 1976, *Ap. J.*, **207**, 367.
Aller, M. F., Aller, H. D., and Hodge, P. E. 1984, preprint.
Angel, J. R. P., and Stockman, H. S. 1980, *Ann. Rev. Astr. Ap.*, **18**, 321.
Avni, Y. 1976, *Ap. J.*, **210**, 642.
Barbieri, C., and Romano, G. 1977, *Acta Astr.*, **27**, 195.
Baylis, W. E., Schmid, W. M., and Lüscher, E. 1967, *Zs. Ap.*, **66**, 271.
Bevington, P. R. 1969, *Data Reduction and Error Analysis for the Physical Sciences* (New York: McGraw-Hill).
Biermann, P., Clarke, J. N., Fricke, K. J., Pauliny-Toth, I. I. K., Schmidt, J., and Witzel, A. 1980, *Astr. Ap.*, **81**, 235.

Blandford, R. D., and Königl, A. 1979, *Ap. J.*, **232**, 34.
Boggess, A., *et al.* 1978*a*, *Nature*, **275**, 372.
———. 1978*b*, *Nature*, **275**, 377.
Bohlin, R. C., and Holm, A. V. 1980, *IUE Newsletter*, **10**, 37.
Bregman, J. N., *et al.* 1982, *Ap. J.*, **253**, 19.
———. 1984, *Ap. J.*, **276**, 454.
Brown, R. L., and Gould, R. J. 1970, *Phys. Rev. D*, **1**, 2252.
Burbidge, G. R., Jones, T. J., and O'Dell, S. L. 1973, *Ap. J.*, **193**, 43.
Burstein, D., and Heiles, C. 1978, *Ap. J.*, **225**, 40.
Cassatella, A., Holm, A., Ponz, D., and Schiffer, F. H. 1980, *IUE Newsletter*, **8**, 1.
Colla, G., Fanti, C., Fanti, R., Gioia, I., Lari, C., Lequeux, J., Lucas, R., and Ulrich, M. H. 1975, *Astr. Ap. Suppl.*, **20**, 1.
Condon, J. J., and Dressel, L. L. 1973, *Ap. Letters*, **15**, 203.
de Bruyn, A. G. 1976, *Astr. Ap.*, **52**, 439.
Forman, W., Jones, C., Cominsky, L., Julien, P., Murray, S., Peters, G., Tananbaum, H., and Giacconi, R. 1978, *Ap. J. Suppl.*, **38**, 357.
Ghigo, F. D., and Owen, F. N. 1973, *A.J.*, **78**, 848.
Giacconi, R., *et al.* 1979, *Ap. J.*, **230**, 540.
Ginzburg, V. L., and Syrovatskii, S. I. 1965, *Ann. Rev. Astr. Ap.*, **3**, 297.
Glassgold, A. E., *et al.* 1983, *Ap. J.*, **274**, 101.
Hackney, R. L., Hackney, K. R., and Kondo, Y. 1982, *Advances in Ultraviolet Astronomy: Four Years of IUE Research*, ed. Y. Kondo, J. M. Mead, and R. D. Chapman (NASA CP-2238), p. 335.
———. 1984, *Future of Ultraviolet Astronomy Based on Six Years of IUE Research*, in press.
Heiles, C. 1975, *Astr. Ap. Suppl.*, **20**, 37.
Hickson, P., Fahlman, G. G., Auman, J. R., Walker, G. A. H., Menon, T. K., and Minkov, Z. 1982, *Ap. J.*, **258**, 53.
Holm, A. 1982, *Advances in Ultraviolet Astronomy: Four Years of IUE Research*, ed. Y. Kondo, J. M. Mead, and R. D. Chapman (NASA CP-2238), p. 339.
Holm, A. V., and Schiffer, F. H. 1980, *IUE Newsletter*, **8**, 45.
Hutter, D. J. 1982, Ph.D. thesis, Indiana University.
Hutter, D. J., and Mufson, S. L. 1981, *A.J.*, **86**, 1585.
Johnson, H. L. 1965, *Ap. J.*, **141**, 923.
Johnson, H. L., Mitchell, R. I., Iriarte, B., and Wiśniewski, W. Z. 1966, *Comm. Lunar and Planet. Lab.*, **4**, 99.
Jones, T. W., O'Dell, S. L., and Stein, W. A. 1974*a*, *Ap. J.*, **188**, 353.
———. 1974*b*, *Ap. J.*, **192**, 261.
Joyce, R. R., and Simon, M. 1976, *Pub. A.S.P.*, **88**, 870.
Kellermann, K. E., and Pauliny-Toth, I. I. K. 1981, *Ann. Rev. Astr. Ap.*, **19**, 373.
Königl, A. 1981, *Ap. J.*, **244**, 700.
Kojoian, G., Sramek, R. A., Dickson, D. F., Tovmassian, H., and Purton, C. R. 1976, *Ap. J.*, **203**, 323.
Kondo, Y., *et al.* 1981, *Ap. J.*, **243**, 690.
Koorneef, J., and de Boer, K. 1979, *IUE Newsletter*, **5**.
Marscher, A. P. 1983, *Ap. J.*, **264**, 296.
Marscher, A. P., Marshall, F. E., Mushotzky, R. F., Dent, W. A., Balonek, T. J., and Hartman, M. F. 1979, *Ap. J.*, **233**, 498.
Maza, J., Martin, P. G., and Angel, J. R. P. 1978, *Ap. J.*, **224**, 368.
McGimsey, B. Q., and Miller, H. R. 1978, *Ap. J.*, **219**, 387.
Mihalas, D., and Binney, J. 1981, *Galactic Astronomy* (San Francisco: Freeman).
Moffet, A. T. 1975, in *Stars and Stellar Systems*, Vol. **9**, *Galaxies and the Universe*, ed. A. Sandage, M. Sandage, and J. Kristian (Chicago: University of Chicago Press), p. 211.
Mufson, S. L., and Hutter, D. J. 1981, *Ap. J. (Letters)*, **248**, L61.
Mushotzky, R. F., Boldt, E. A., Holt, S. S., Pravdo, S. H., Serlemitsos, P. J., Swank, J. H., and Rothschild, R. H. 1978, *Ap. J. (Letters)*, **226**, L65.
Osterbrock, D. E. 1978, *Proc. Nat. Acad. Sci.*, **75**, 540.
Owen, F. N., Porcas, R. W., Mufson, S. L., and Moffett, T. J. 1978, *A.J.*, **83**, 685.
Owen, F. N., Spangler, S. R., and Cotten, W. D. 1980, *A.J.*, **85**, 351.
Panek, R. J. 1983, *IUE Newsletter*, **21**, 43.
Rees, M. J. 1977, *Ann. NY Acad. Sci.*, **302**, 613.
Rees, M. J., Begelman, M. C., and Blandford, R. D. 1981, *Ann. NY Acad. Sci.*, **357**, 254.
Sandage, A. 1973, *Ap. J.*, **180**, 691.
———. 1975, in *Stars and Stellar Systems*, Vol. **9**, *Galaxies and the Universe*, ed. A. Sandage, M. Sandage, and J. Kristian (Chicago: University of Chicago Press), p. 761.
Schwartz, D. A., Bradt, H. V., Doxsey, R. E., Griffiths, R. E., Gursky, H., Johnston, M. D., and Schwartz, J. 1978, *Ap. J. (Letters)*, **224**, L103.
Snijders, M. J. A., Boksenberg, A., Bass, P., Sanford, P. W., Ives, J. C., and Penston, M. V. 1979, *M.N.R.A.S.*, **189**, 873.
Sramek, R. A., and Tovmassian, H. M. 1975, *Ap. J.*, **196**, 339.
Sulentic, J. W. 1976, *A.J.*, **81**, 582.
Turnrose, B. E., and Harvel, C. A. 1980, *IUE Image Processing Information Manual*, Version 1.0, 6-6.
Ulrich, M. H. 1978*a*, in *Pittsburgh Conference on BL Lac Objects*, ed. A. M. Wolfe (Pittsburgh: University of Pittsburgh Press), p. 192.
Ulrich, M. H., Hackney, K. R. H., Hackney, R. L., and Kondo, Y. 1984, *Ap. J.*, **276**, 466.
Ulrich, M. H., Kinman, T. D., Lynds, C. R., Rieke, G. H., and Ekers, R. D. 1975, *Ap. J.*, **198**, 261.
Urry, C. M., and Mushotzky, R. M. 1982, *Ap. J.*, **253**, 38.
Urry, C. M., and Mushotzky, R. M., Kondo, Y., Hackney, K. R. H., and Hackney, R. L. 1982, *Ap. J.*, **261**, 12.
Weiler, K. W., and Johnston, K. J. 1980, *M.N.R.A.S.*, **190**, 269.
Whitford, A. E. 1975, in *Stars and Stellar Systems*, Vol. **9**, *Galaxies and the Universe*, ed. A. Sandage, M. Sandage, and J. Kristian (Chicago: University of Chicago Press), p. 159.
Worrall, D. M., Boldt, E. A., Holt, S. S., Mushotzky, R. F., and Serlemitsos, R. J. 1981, *Ap. J.*, **243**, 53.

H. D. Aller, M. F. Aller, and P. E. Hodge: Department of Astronomy, University of Michigan, 953 Physics-Astronomy Building, Ann Arbor, MI 48109

K. R. Hackney and R. L. Hackney: Department of Physics and Astronomy, Western Kentucky University, TCCW, Bowling Green, KY 42101

D. J. Hutter: Department of Physics and Astronomy, Georgia State University, Atlanta, GA 30303

Y. Kondo: Laboratory for Astronomy and Solar Physics, NASA/Goddard Space Flight Center, Code 685, Greenbelt, MD 20771

S. L. Mufson: Department of Astronomy, Indiana University, 319 Swain West, Bloomington, IN 47405

R. F. Mushotzky and C. M. Urry: Laboratory for High Energy Astrophysics, NASA/Goddard Space Flight Center, Code 661, Greenbelt, MD 20771

W. Z. Wiśniewski: Lunar and Planetary Laboratory, University of Arizona, Tucson, AZ 85721